



# CHORUS

This is the accepted manuscript made available via CHORUS. The article has been published as:

## Quantum electron lifetime in GaAs quantum wells with three populated subbands

Scott Dietrich, Jesse Kanter, William Mayer, Sergey Vitkalov, D. V. Dmitriev, and A. A. Bykov

Phys. Rev. B **92**, 155411 — Published 8 October 2015

DOI: [10.1103/PhysRevB.92.155411](https://doi.org/10.1103/PhysRevB.92.155411)

# Quantum electron lifetime in GaAs quantum wells with three populated subbands.

Scott Dietrich, Jesse Kanter, William Mayer, and Sergey Vitkalov\*  
*Physics Department, City College of the City University of New York, New York 10031, USA*

D. V. Dmitriev  
*A.V.Rzhanov Institute of Semiconductor Physics, Novosibirsk 630090, Russia*

A. A. Bykov  
*A.V.Rzhanov Institute of Semiconductor Physics, Novosibirsk 630090, Russia and  
Novosibirsk State University, Novosibirsk 630090, Russia*  
(Dated: September 22, 2015)

The magnetotransport of highly mobile 2D electrons is studied in GaAs single quantum wells with three occupied subbands. The bottoms of the lower two subbands have nearly the same energy while the bottom of the third subband has a much higher energy ( $E_1 \approx E_2 \ll E_3$ ). Magnetointersubband oscillations (MISO) between the  $i^{\text{th}}$  and  $j^{\text{th}}$  subbands are observed and obey the relation  $\Delta_{ij} = E_j - E_i = l \cdot \hbar\omega_c$ , where  $\omega_c$  is the cyclotron frequency and  $l$  is an integer. The slight difference in the energies of the lower subbands produces noticeable interference effects in the magnetoresistance. In contrast to the case of two populated subbands, by analyzing the amplitude of each component of the MISOs separately, the quantum lifetime  $\tau_q^{(i)}$  of electrons in  $i^{\text{th}}$  subband is extracted. The studies show that  $\tau_q^{(1)} \approx \tau_q^{(2)} = \tau_q^{(1,2)}$ . The temperature variation of  $1/\tau_q^{(1,2)}$  is found to be proportional to  $T^2$  indicating that the electron-electron interaction is the dominant source of the decrease of the electron lifetime at high temperatures. Different temperature dependence of the quantum scattering rate is found in the third subband,  $\delta(1/\tau_q^{(3)}) \sim T$ , which is consistent with the theory of sparsely populated subbands.

## I. INTRODUCTION

The quantization of electron motion in magnetic fields generates an abundance of fascinating phenomena observed in condensed materials<sup>1</sup>. One of the most famous examples is the Shubnikov-de Haas (SdH) resistance oscillations. The passage of strongly degenerate Landau levels through the Fermi surface at a low temperature  $T$  produces resistance oscillations due to a modulation of the net number of electron states in the energy interval  $kT < \hbar\omega_c$  near the Fermi energy  $E_F$  that provide the dominant contribution to electron transport<sup>2,3</sup>. The SdH oscillations are periodic in the inverse magnetic field ( $1/B$ ) and correspond to the condition  $E_F = l \cdot \hbar\omega_c$ . At  $kT > \hbar\omega_c$ , the amplitude of SdH oscillations is strongly suppressed due to the averaging of oscillations in the density of states (DOS) within the interval  $kT$ . In two dimensional electron systems, SdH oscillations can be very pronounced<sup>2</sup>, leading to the Quantum Hall Effect (QHE) at low temperatures  $kT \ll \hbar\omega_c$ <sup>4</sup>. The QHE is related to the strong quantization (discreteness) of the electron spectrum in high magnetic fields,  $\hbar\omega_c > \Gamma$ , in which the separation of Landau levels ( $\hbar\omega_c$ ) is larger than the level broadening ( $\Gamma = \hbar/\tau_q$ ).

Landau quantization produces remarkably strong effect on Joule heating of two dimensional (2D) electrons<sup>5-8</sup>. The heating forces 2D electrons into exotic electronic states in which voltage (current) does not depend on current<sup>9-11</sup> (voltage<sup>12</sup>). Joule heating provides a particularly noticeable effect on 2D electron transport at magnetic fields corresponding to strong quantization,

$\hbar\omega_c > \Gamma$ . In contrast to linear response at low temperatures  $kT \ll \hbar\omega_c$  (QHE), Joule heating is affected by the quantization in a significantly broader temperature range. At  $\hbar\omega_c > \Gamma$  and  $kT \gg \hbar\omega_c$  the *dc* heating produces a remarkable multi-tiered electron distribution containing as many tiers as the number of Landau levels inside the energy interval  $kT$ :  $N \approx kT/\hbar\omega_c$ . This quantal heating preserves the overall broadening ( $\sim kT$ ) of the electron distribution<sup>7,13</sup>. Joule heating is considered to be one of the main sources of the broad variety of strongly nonlinear phenomena found in the frequency range from dc to THz and presenting an exciting area of contemporary research<sup>14</sup>.

Two-dimensional electron systems with multiple populated subbands exhibit a different kind of quantum magnetoresistance oscillations<sup>15-22</sup>. These magneto-inter-subband oscillations (MISO) of the resistance are due to the alignment between Landau levels from different subbands  $i$  and  $j$  with corresponding energies  $E_i$  and  $E_j$ . Resistance maxima occur at magnetic fields at which the gap between the bottoms of subbands,  $\Delta_{ij} = E_i - E_j$ , equals a multiple of the Landau level spacing,  $\hbar\omega_c$ :  $\Delta_{ij} = l \cdot \hbar\omega_c$ , where  $l$  is an integer<sup>23-26</sup>. At this condition electron scattering on rigid impurities is enhanced due to the possibility of electron transitions between  $i^{\text{th}}$  and  $j^{\text{th}}$  subbands. At magnetic fields corresponding to the condition  $\Delta_{ij} = (l+1/2) \cdot \hbar\omega_c$  the intersubband electron transitions are suppressed. As a result, the resistance oscillates periodically in inverse magnetic field due to the modulation of the electron scattering. In contrast to SdH oscillations MIS oscillations are resilient to the total number of the quantum states responsible for the

electron transport (states inside the  $kT$  interval near the Fermi level,  $E_F$ ) and, thus, are significantly less sensitive to the temperature. The MISO are observed at high temperatures,  $kT \gg \hbar\omega_c$  at which SdH oscillations (and QHE) are absent. The temperature dependence of the MISO amplitude is due to the temperature broadening of Landau levels or, in other words, due to the temperature dependence of the quantum scattering time  $\tau_q(T)$ .

A theoretical analysis yields the following expression for the amplitude of MISO due to the scattering between the  $i^{\text{th}}$  and  $j^{\text{th}}$  subbands<sup>25,26</sup>:

$$\Delta\rho_{MISO}^{(i,j)} = \frac{2m \cdot \nu_{ij}}{e^2(n_i + n_j)} \cdot \cos\left(\frac{2\pi\Delta_{ij}}{\hbar\omega_c}\right) \times \exp\left[\frac{-\pi}{\omega_c}\left(1/\tau_q^{(i)} + 1/\tau_q^{(j)}\right)\right], \quad (1)$$

where  $n_i$  and  $m$  are the electron density and the effective mass in the  $i^{\text{th}}$  subband and  $\nu_{ij}$  is an effective intersubband scattering rate<sup>26</sup>. This expression has recently been used in systems with two populated subbands to extract the total scattering rate  $1/\tau_q = 1/\tau_q^{(1)} + 1/\tau_q^{(2)}$ <sup>17-22</sup>. However, fitting the amplitude of MISO to this function cannot give the scattering rate of each subband separately unless additional relations are used. In particular for two subbands with nearly equal electron population  $n_1 \approx n_2$ , theory suggests that the rates are approximately equal:  $1/\tau_q^{(1)} \approx 1/\tau_q^{(2)}$ <sup>17-20,26</sup>. In this paper we show that the quantum electron lifetimes in nearly equally populated subbands are, indeed, very close to each other.

For three populated subbands there are three different MISOs corresponding to the scattering between different subbands. In accordance with Eq.(1) there are three relations for the products of Dingle factors  $d_i = \exp(-\pi/\omega_c\tau_q^{(i)})$  allowing separation of the electron quantum lifetime  $\tau_q^i$  for each subband.

Recently MISO have been studied in GaAs quantum wells with three populated subbands at high temperatures, at which the third subband is thermally populated<sup>28</sup>. The thermal population of a subband makes the quantitative study of the temperature dependence of the quantum scattering time in this subband to be quite challenging. The direct evaluation of the scattering rate based on Eq.(1) was obscured by the strong exponential increase of the third subband population. The Authors have developed a theory, predicting the temperature variations of the scattering rate to be  $\sim T$  in the third subband and have demonstrated that the observed temperature dependence of the amplitude of MISO is in fair agreement with the theoretical prediction. However the presented variations of the MISO amplitude (blue and red symbols in Fig.3<sup>28</sup>) are also compatible with the  $T^2$  temperature variation of the quantum scattering rate in the third subband at high temperatures making the obtained results to be inconclusive.

In this manuscript, we present the study of GaAs single quantum wells when three subbands are populated at low

temperatures with the relation  $E_1 \approx E_2 \ll E_3 < E_F$  between the bottom energies of the subbands. The electron densities in the lower two subbands are, thus, approximately equal and are substantially larger than the one in the highest subband. Our samples demonstrate strong MISO in a wide range of temperatures yielding the quantum scattering rate regardless of the temperature variations of the rate. The analysis of MISOs indicates that the quantum scattering times obey the following relation  $\tau_q^{(1)}(T) \approx \tau_q^{(2)}(T)$  and demonstrates different temperature dependencies for the lower [ $\delta(1/\tau_q^{(1,2)}) \sim T^2$ ] and the upper [ $\delta(1/\tau_q^{(3)}) \sim T$ ] subbands.

## II. EXPERIMENTAL SETUP

Highly mobile GaAs quantum wells were grown by molecular beam epitaxy on a semi-insulating (001) GaAs substrate. The material was fabricated from a selectively doped GaAs single quantum well (56 nm) sandwiched between AlAs/GaAs superlattice barriers. The heterostructure was designed to create three populated subbands with energies at the bottoms of the subbands  $E_1$ ,  $E_2$ , and  $E_3$  such that  $E_1 \approx E_2 \ll E_3$ . The subband energies are schematically shown in the insert to Figure 1.

The studied samples were etched in the shape of a Hall bar. The width and the length of the measured part of the samples are  $W = 50\mu\text{m}$  and  $L = 250\mu\text{m}$ . AuGe eutectic was used to provide electric contacts to the 2D electron gas. The samples were studied at different temperatures from 2 to 9 Kelvin in magnetic fields up to 0.6 Tesla applied perpendicular to the 2D layer. The total electron density of samples,  $n_T \approx 8.6 \times 10^{11} \text{cm}^{-2}$ , was evaluated from Hall measurements at high magnetic field. An average electron mobility  $\mu \approx 1.6 \times 10^6 \text{cm}^2/\text{Vs}$  was obtained from  $n_T$  and the zero-field resistivity around  $T = 4.6\text{K}$ . Sample resistance was measured using the four-point probe method. We applied a 12Hz *ac* excitation ( $I_{ac}$ ) through the current contacts and measured the longitudinal and Hall *ac* voltages ( $V_{xx}^{ac}$  and  $V_H^{ac}$ ) using two lockin amplifiers with 10M $\Omega$  input impedances. The potential contacts provided insignificant contribution to the overall response due to small values of the contact resistance (about 1k $\Omega$ ) and negligibly small electric current flowing through the contacts. The measurements were done in the linear regime, when the voltages are proportional to the applied current. Six samples have been studied demonstrating similar temperature dependencies for lower and upper subbands. The manuscript presents data for three samples A, B and C.

## III. RESULTS AND DISCUSSION

Figure 1a presents the longitudinal resistivity,  $\rho_{xx}(B)$ , of samples A, B and C. In accordance with Eq.(1) the frequency of MIS oscillations in the inverse mag-

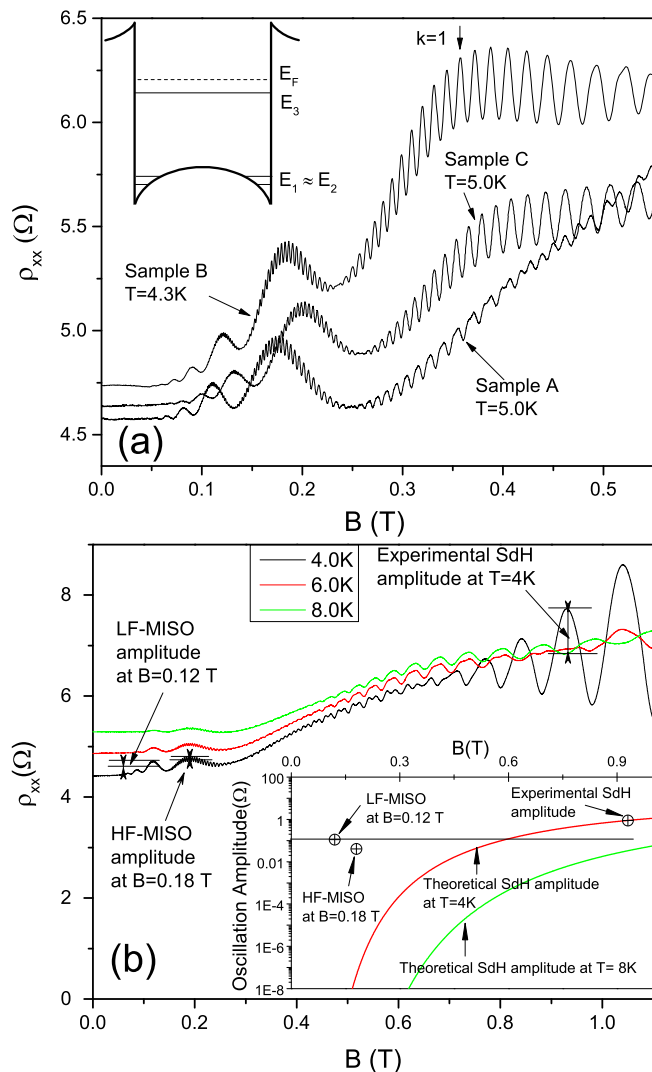


FIG. 1: (a) Magnetoresistivity of samples A, B and C at different temperatures as labeled. The inset shows the energy diagram of the quantum well with three occupied subbands, where  $E_1$ ,  $E_2$ , and  $E_3$  designate the energy of the bottom of each subband and  $E_F$  designates the Fermi energy. (b) Magnetoresistivity of samples A at different temperatures. SdH oscillations are developed at  $T=4\text{K}$  in magnetic fields above 0.6 T. Insert presents comparison of the amplitude of quantum oscillations at small ( $B=0.12\text{ T}$ ) and high magnetic fields with the amplitude of SdH oscillations at different temperatures expected from theory<sup>27</sup>.

netic field is proportional to the intersubband energy gap ( $f_{ij} \propto \Delta_{ij} = E_i - E_j$ ). This three subband system should therefore have MISOs at three different frequencies, corresponding to resonant scattering between the three subbands. MISOs associated with scattering between the lowest two subbands will have a low frequency (LF-MISO),  $f_{21} \propto E_2 - E_1$ , since the energy spacing  $\Delta_{21}$  is very small ( $E_1 \approx E_2$ ). The two sets of MISOs associated with scattering between the upper band and each of the lower bands will have much

higher frequencies (HF-MISO) that are approximately equal since  $\Delta_{31} \approx \Delta_{32} \gg \Delta_{21}$ . Due to the small difference between energy  $E_1$  and  $E_2$  the interference between these two sets produces a beating pattern between two frequencies  $f_{31}$  and  $f_{32}$  with a small beating frequency  $f_{beat} \propto (E_2 - E_1)/2 \ll f_{3i}$  and a high inner frequency  $f_{avg} \propto (2E_3 - E_2 - E_1)/2$ . The presence of resistance oscillations with both the low ( $f_{21}$ ) and high ( $f_{31}, f_{32}$ ) frequencies is shown in Figure 1a.

Figure 1b presents the longitudinal resistivity,  $\rho_{xx}(B)$ , in a broader range of magnetic fields at different temperatures as labeled. At temperature  $T = 4\text{ K}$  and magnetic fields above 0.6 T a significant increase of the amplitude of quantum oscillations is observed. At these conditions the cyclotron energy exceeds the broadening of the electron distribution ( $\sim kT$ ) and the contribution of Shubnikov de Haas (SdH) oscillations to the oscillating content of the magnetoresistance dominates. The SdH oscillations have strong temperature and magnetic field dependencies and are absent at small magnetic fields and/or high temperatures. The insert to Fig.1b presents the expected amplitude of SdH oscillations obtained using the following expression<sup>27</sup>:

$$\Delta\rho_{xx} = 2\rho_D \frac{2\pi^2 kT/\hbar\omega_c}{\sinh(2\pi^2 kT/\hbar\omega_c)} \exp\left(-\frac{\pi}{\omega_c\tau_q}\right), \quad (2)$$

where  $\rho_D$  is Drude resistivity. Experimental values of the amplitude of quantum oscillations are depicted in the insert as symbols and show good agreement with this expression at high magnetic fields. However, the amplitude of observed oscillations at small magnetic fields ( $B=0.12\text{ T}$ ,  $B=0.18\text{ T}$ ) is more than 6 orders of magnitude larger than the expected amplitude of SdH oscillations. This observation clearly indicates that contribution of the SdH oscillations in the oscillating content of the magnetoresistance is negligibly small at weak magnetic fields. The SdH contribution is neglected in the comparison of the quantum oscillations observed at  $B < 0.3\text{ T}$  with the existing theory of MISO.

Due to a precise relation between different frequencies the beating frequency is twice less the frequency of MISO corresponding to the two lower subbands:  $f_{beat} = f_{21}/2$ . This is indeed seen in Figure 2. Figure 2 presents the magnetoresistivity for two temperatures as labeled. The magnetoresistivity demonstrates oscillations at several frequencies. The figure shows the expected exact relation between the low frequency oscillations (LF-MISO) and the beating between two high frequency (HF) MISOs. Namely the maximal amplitude of the HF-MISO is achieved at the maxima of LF-MISO while the minimal amplitude of HF-MISO (node) corresponds to the minima of LF-MISO. An accurate analysis of the positions of HF-MISO indicates a phase shift by  $\pi$  between the HF-MISO maxima located at different sides of a beating node. It confirms the relation,  $f_{beat} = f_{21}/2$ , expected between the frequency of the LF-MISO and the beating frequency.

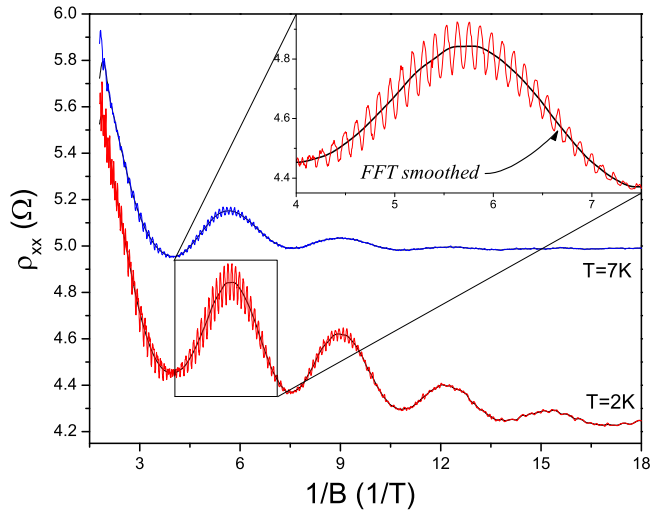


FIG. 2: (Color online) Magnetoresistivity at two temperatures as labeled (blue and red curves). Black curves present the results of FFT filtering. The inset shows one period of slow oscillations for the  $T=2\text{K}$  data, which matches with the beating period of the fast oscillations. Sample A.

The significant frequency difference between the low and high frequency contents facilitate the separation of HF and LF MISOs by an application of frequency filtering. In Figure 2 black thick curves represent results of a fast Fourier transform (FFT) filtering that has been applied to  $\rho_{xx}(1/B)$  yielding the slow oscillations. The inset shows one period of the FFT filtered low frequency content, which corresponds to LF-MISO with frequency  $f_{21}$ . Fast oscillations clearly demonstrate a beat pattern which shares nodes with the minima of the slow oscillation. A subtraction of the slowly varying component from the original data yields the fast oscillations. Figure 3 presents the separated components of the magnetoresistance oscillations corresponding to low (Figure 3a) and high (Figure 3b-3h) frequencies at different temperatures.

A comparison of the curves obtained at different temperatures shows that the amplitude of both HF- and LF-MISOs is decreases considerably at higher temperatures. This is mostly due to the decrease of the electron quantum lifetime  $\tau_q^{(i)}(T)$  at high temperatures. The observed evolution of MISO with the temperature allows for the study of the temperature dependence of the  $\tau_q^{(i)}(T)$  in different subbands.

Figure 4 shows the results of fitting the LF- and HF-MISO data to Eq. (1). The fitting functions used for each type of oscillations are shown in each figure respectively. Figure 4(a) shows the comparison of LF-MISO corresponding to the scattering between two lower subbands (1,2) with the theory. The LF-MISO ( $\Delta\rho_{12}$ ) were obtained by subtracting a monotonic background of the magnetoresistance  $\rho_{slow}$  shown in the insert to the figure. The background magnetoresistance has been removed by subtracting an average of the MISO envelope shown in the inset. The envelope was obtained by cubic spline

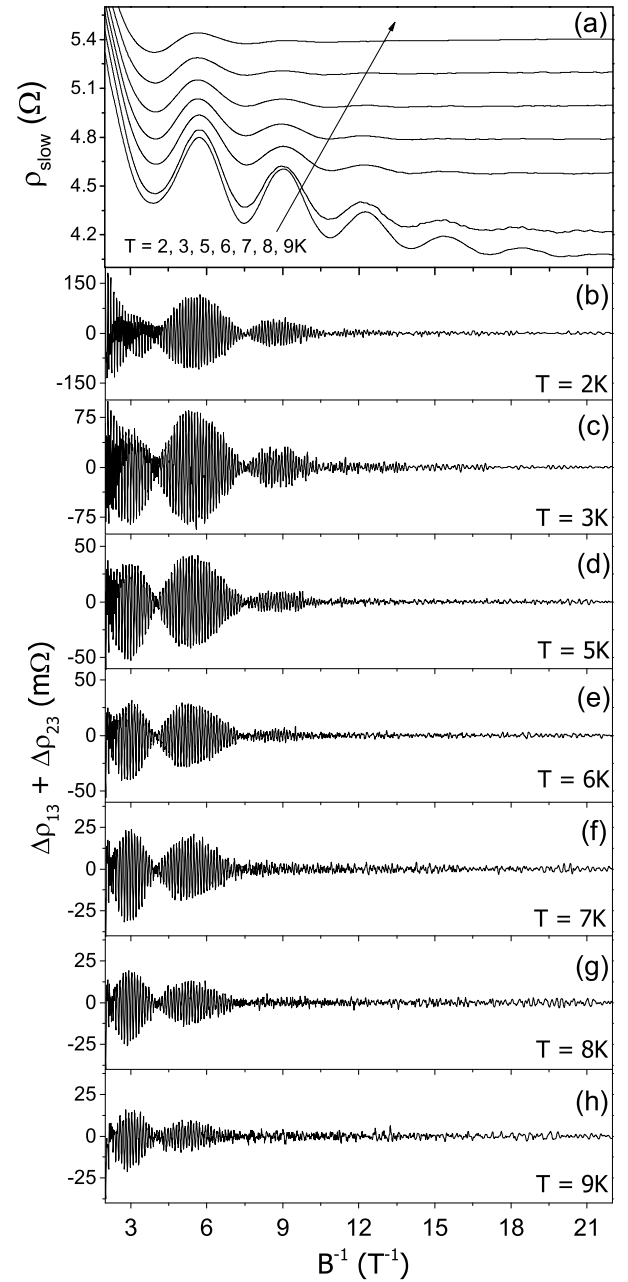


FIG. 3: Shown above are the low (a) and high frequency (b-h) components of the magnetoresistivity separated by FFT filtering. (a) The slowly varying magnetoresistivity,  $\rho_{slow}(1/B)$ , contains the background magnetoresistivity and contributions from intersubband scattering between the lower two subbands. (b-h) Fast oscillations in the magnetoresistivity,  $\Delta\rho_{13} + \Delta\rho_{23}$ , come from intersubband scattering between the upper subband and the two lower subbands. Sample A.

between minima and maxima of the experimental data. Fitting the LF-MISO data uses an expression corresponding to Eq. (1) for  $\Delta\rho_{12}$ , while the shown in Fig. 4(b) fit of HF-MISO data uses an expression corresponding to sum of two MISOs,  $\Delta\rho_{13} + \Delta\rho_{23}$ , describing scattering from lower subbands (1,2) and the third subband. The

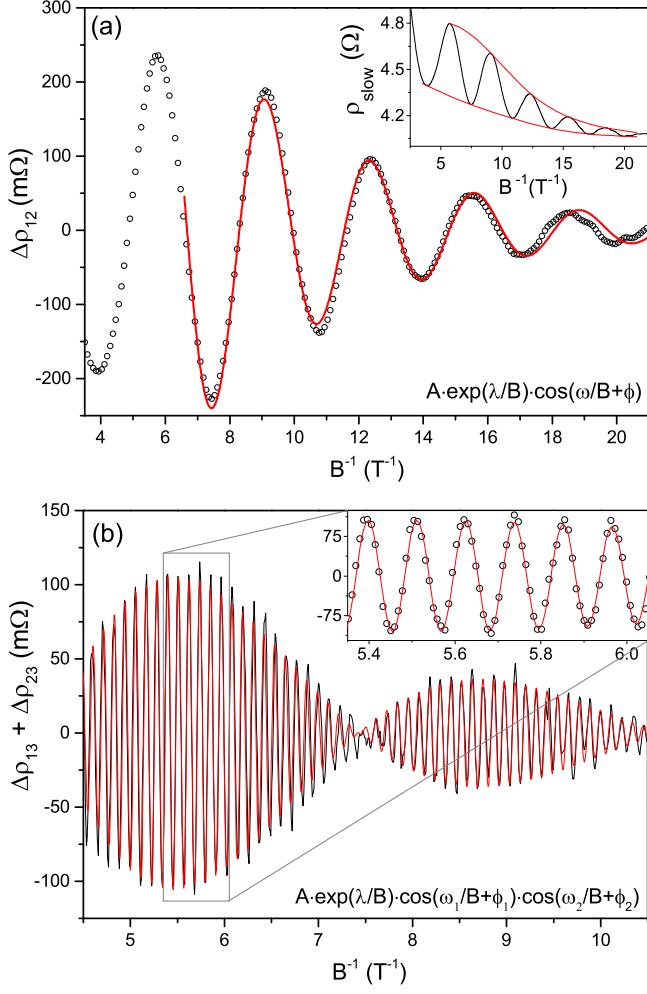


FIG. 4: (Color online) Shown above are examples of fitting the low (a) and high (b) frequency MIS oscillations with the equations shown. Red curves depict the fitting while black curves and open circles represent experimental data from Sample A at  $T = 2\text{K}$ . Obtained fitting parameters are for (a) LF-MISO:  $A=1.038$  (Ohm),  $\lambda=-0.196$  (T),  $\omega=1.929$  (T),  $\phi=1.26$  (rad); (b) HF-MISO:  $A=0.67$  (Ohm),  $\lambda=-0.327$  (T),  $\omega_1=0.968$  (T),  $\phi_1=0.66$  (rad),  $\omega_2=55.31$  (T),  $\phi_2=3.06$  (rad).

theoretical expressions are valid at small magnetic fields, at which the product of Dingle factors  $d_i d_j$  is small<sup>26</sup>. In practice an exponentially growing with reciprocal magnetic field,  $1/B$ , oscillating part of the magnetoresistance is used to extract the quantum scattering time keeping the fitting function inside the range of small magnetic fields.

The HF-MISO fitting function (product of two cosines) follows from assumptions that (a) the scattering rate between first and third subbands is identical to the scattering rate between second and third subbands and (b) the quantum scattering rates in lower subbands are identical. The almost perfect agreement between the fitting function and the experiment indicates the validity of these assumptions which have been used for the interpretation

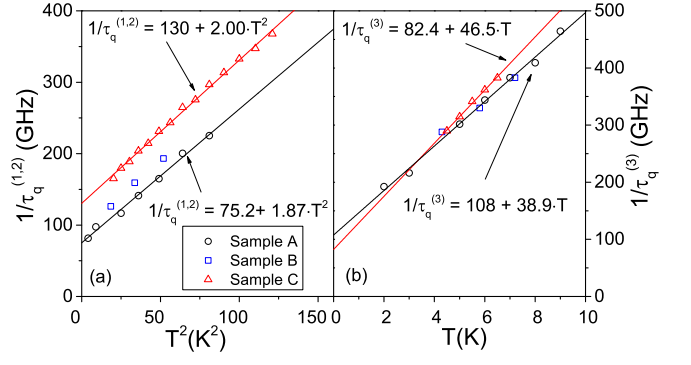


FIG. 5: (a) Temperature dependence of quantum scattering rate in the lower two subbands,  $1/\tau_q^{(1,2)} \sim T^2$  indicates that the electron-electron scattering is the main source limiting the electron lifetime at high temperatures; (b) the quantum scattering rate in third subband  $1/\tau_q^{(3)}$ , demonstrates a linear dependence on the temperature, which is compatible with theory of electron-electron scattering in sparsely populated bands.<sup>28</sup>

of previous experiments<sup>17,20,28</sup>.

The exponential decay parameter,  $\lambda$ , is used to extract the quantum scattering rates and the frequencies  $\omega_i$  are used to measure the intersubband energy separations  $\Delta_{ij}$ . Frequencies extracted from the fitting,  $f_{beat} = \omega_1/2\pi = f_{21}/2 = (m/\hbar e)(\Delta_{31} - \Delta_{32})/2 = 0.154\text{T}$  and  $f_{avg} = \omega_2/2\pi = (m/\hbar e)(\Delta_{31} + \Delta_{32})/2 = 8.803\text{T}$ , confirm that the gap between the lower two subbands,  $\Delta_{21} = 0.53$  meV, is much less than the one between the uppermost and the lowest subbands,  $\Delta_{31} = 15.48\text{meV}$ . Additionally,  $f_{21}$  extracted from the LF-MISOs was consistent with those extracted from the beating of HF-MISOs. These subband gaps and the total electron density,  $n_T$ , give a Fermi energy,  $E_F = 15.58\text{meV}$ , just above the third subband. Here, energies are referenced from the bottom of the lowest subband,  $E_1$ . Since  $E_3$  is very close to  $E_F$  the frequencies of Shubnikov de Haas (SdH) oscillations from the two lowest subbands  $\omega_{(1,2)}^{SdH} \sim (E_F - E_{1,2})$  are very close to the corresponding frequencies of HF-MISO. This is indeed found in our samples. Furthermore the phase of SdH oscillations demonstrates a shift by 180 degree with respect to HF-MISO similar to what has been seen earlier in two subband systems<sup>30</sup>.

In accordance with Eq.(1) the exponential decay parameter,  $\lambda$ , gives the total quantum scattering rate. The deep nodes observed for HF-MISO indicate that the quantum scattering rates in lower subbands are nearly identical:  $\tau_q^{(1)} \approx \tau_q^{(2)}$ . Thus, the argument in the exponent of Eq. (1) describing LF-MISO becomes  $2\pi/\omega_c \tau_q^{(1,2)}$  and the exact quantum scattering rate  $1/\tau_q^{(1,2)}$  can be obtained through fitting. These results are shown in Figure 5(a) for different samples as labeled.

Figure 5(b) shows the scattering rate,  $1/\tau_q^{(3)}$  in third subband obtained from fitting of the HF-MISO. For these oscillations, the total scattering rate, obtained from fit-

ting, contains the quantum scattering rate of the lower two subbands as well as that of the third subband. Figure 5(b) shows the result of the subtraction of the quantum scattering rate of the lower two bands,  $1/\tau_q^{(1,2)}$  from the total rate yielding the quantum scattering rate of electrons in the third subband,  $1/\tau_q^{(3)}$ .

Shown in Figure 5(a) the temperature variations of the quantum scattering rate,  $1/\tau_q^{(1,2)}$  are proportional to  $T^2$  indicating that electron-electron scattering is the dominant mechanism limiting the electron lifetime in the lower two subbands at high temperature. This result is in a good agreement with previous studies of highly populated subbands<sup>17,20,29</sup>. The upper subband demonstrates a different temperature dependence of the quantum scattering rate as shown in Figure 5(b). Despite a comparable variation of the scattering rate in different subbands in the studied temperature range, the variation of the rate in third subband is more compatible with a linear temperature dependence:  $\delta(1/\tau_q^{(3)}) \sim T$ . The linear dependence is in agreement with theoretical estimations of the strength of  $e - e$  scattering in subbands with a low electron population<sup>28</sup>.

While in all studied samples the magnetoresistance is found to be similar at small magnetic fields, a complex behavior of the magnetoresistance is observed at high magnetic fields corresponding to the condition  $\Delta_{12} \approx \hbar\omega_c$ . The behavior of the magnetoresistance is found to be considerably different in different samples. The effect is clearly seen in Figure 1. While Sample B shows all peaks corresponding to LF-MISO:  $\Delta_{12} = k \cdot \hbar\omega_c$ , sample A does not indicate any considerable enhancement of the scattering between two lowest subbands at  $k=1$ . The effect is accompanied by a significant reduction of the HF-MISO amplitude in the corresponding magnetic field range. We note that the decrease of the low indexed LF-MISO has been also observed in samples with 2D electrons, which were thermally activated into the third subband<sup>28</sup>. The authors have suggested that the effect could be associated with some mechanisms of Landau-level broadening not taken into account or with the influence of electron-phonon scattering on magnetotransport. Our measurements indicate that the behavior of samples with almost identical properties is different only in a particular range of magnetic fields when the cyclotron energy  $\hbar\omega_c$  is comparable with the lower subband separation,  $\Delta_{12}$ :  $\Delta_{12} \approx \hbar\omega_c$ . It points toward an instability (or flexibility) of the electron spectrum at this conditions in a wide quantum wells. It is interesting to note that a considerable variation of the subband separation with the filling factor has been seen in quantum wells with an asymmetric doping<sup>31,32</sup>. A significant modification of the properties of QHE, in particular quantized 5/2 state, has been observed with the widening quan-

tum wells<sup>33-35</sup>. These phenomena indicate an important role of the electrostatic re-population of the subbands in wide quantum wells placed in the quantizing magnetic fields. It is realized recently that the re-population could be significantly enhanced in quantum wells grown inside screening superlattices<sup>36-38</sup>. These quantum wells were used in the presented research. We suggest that the absence of the  $k=1$  LF-MISO peak and significant reduction of HF-MISO magnitude at the same range of magnetic field could be related to a modification of the subband separation due to the breaking inversion symmetry of the symmetrically doped quantum wells induced by strong magnetic fields. The corresponding intersubband charge redistribution may decrease the subband energy gap as well as the overlap of the subband wavefunctions. The latter directly effects the rate of intersubband scattering. Another possibility of the strong modification of MISO spectrum at high magnetic fields is due to effect of in-plane magnetic field, which may be present in the experiments due to a small misalignment of samples in magnetic fields. A significant modification of the spectrum of Shubnikov -de Haas oscillations by in-plane magnetic field has been reported recently<sup>39</sup>. All these proposals require further systematic investigations.

#### IV. CONCLUSION

Magneto-inter-subband oscillations of longitudinal resistance has been studied in wide quantum wells with three subbands populated at different temperature. MISO with three different periods in reciprocal magnetic field are observed and indicate that the energy separation between the bottoms of lower subbands  $\Delta_{12} = E_2 - E_1$  is much smaller than the separation between the lower (1,2) and topmost (3) subbands:  $\Delta_{13}, \Delta_{23}$ . Analysis of the magnitude of different MISOs indicates that the intersubband scattering rate between the lower and topmost subbands ( $\nu_{13}$  and  $\nu_{23}$ ) and the quantum electron lifetimes in the lower subbands ( $\tau_q^{(1)}$  and  $\tau_q^{(2)}$ ) are nearly the same. The temperature dependence of the quantum scattering rate is found to be proportional to square of the temperature in lower subbands. The temperature dependence in the significantly less populated upper subband is more compatible with the linear temperature dependence. The obtained temperature dependencies are in accord with existing theory indicating  $e - e$  scattering as the dominant mechanism limiting the electron lifetime.

This work was supported by the National Science Foundation (Division of Material Research - 1104503), the Russian Foundation for Basic Research (project no.14-02-01158) and the Ministry of Education and Science of the Russian Federation.

---

\* Corresponding author: vitkalov@sci.cuny.cuny.edu

<sup>1</sup> D. Shoenberg *Magnetic oscillations in metals*, (Cambridge

- University Press, 1984).
- <sup>2</sup> T. Ando, A. B. Fowler, and F. Stern, *Rev. of Mod. Phys.* B **54**, 437 (1982).
  - <sup>3</sup> J. M. Ziman *Principles of the theory of solids*, (Cambridge at the University Press, 1972).
  - <sup>4</sup> Sankar D. Sarma, Aron Pinczuk *Perspectives in Quantum Hall Effects*, (Wiley-VCH, Weinheim, 2004).
  - <sup>5</sup> I. A. Dmitriev, M.G. Vavilov, I. L. Aleiner, A. D. Mirlin, and D. G. Polyakov, *Phys. Rev. B* **71**, 115316 (2005).
  - <sup>6</sup> Jing-qiao Zhang, Sergey Vitkalov, A. A. Bykov, A. K. Kalagin, and A. K. Bakarov *Phys. Rev. B* **75**, 081305(R) (2007).
  - <sup>7</sup> Jing Qiao Zhang, Sergey Vitkalov, and A. A. Bykov *Phys. Rev. B* **80**, 045310 (2009).
  - <sup>8</sup> N. C. Mamani, G. M. Gusev, O. E. Raichev, T. E. Lamas, and A. K. Bakarov, *Phys. Rev. B* **80**, 075308 (2009).
  - <sup>9</sup> A. A. Bykov, Jing-qiao Zhang, Sergey Vitkalov, A. K. Kalagin, and A. K. Bakarov *Phys. Rev. Lett.* **99**, 116801 (2007).
  - <sup>10</sup> W. Zhang, M. A. Zudov, L.N. Pfeiffer, and K.W. West, *Phys. Rev. Lett.* **100**, 036805 (2008).
  - <sup>11</sup> G. M. Gusev, S. Wiedmann, O. E. Raichev, A. K. Bakarov, and J. C. Portal *Phys. Rev. B* **83**, 041306 (2011).
  - <sup>12</sup> A. A. Bykov, Sean Byrnes, Scott Dietrich, Sergey Vitkalov, I. V. Marchishin and D. V. Dmitriev, *Phys. Rev. B* **87**, 081409(R) (2013).
  - <sup>13</sup> N. R. Kalmanovitz, A. A. Bykov, S. Vitkalov, and A. I. Toropov *Phys. Rev. B* **78**, 085306 (2008).
  - <sup>14</sup> I. A. Dmitriev, A. D. Mirlin, D. G. Polyakov, M. A. Zudov, *Rev. Mod. Phys.* **84**, 1709 (2012).
  - <sup>15</sup> P. T. Coleridge, *Semicond. Sci. Technol.* **5**, 961 (1990).
  - <sup>16</sup> D. R. Leadley, R. Fletcher, R. J. Nicholas, F. Tao, C. T. Foxon, and J. J. Harris, *Phys. Rev. B* **46**, 12439 (1992).
  - <sup>17</sup> A. A. Bykov, D. R. Islamov, A. V. Goran, A. I. Toropov, *JETP Lett.* **87**, 477 (2008).
  - <sup>18</sup> A. A. Bykov, *JETP Lett.* **88**, 64 (2008).
  - <sup>19</sup> A. A. Bykov, *JETP Lett.* **88**, 394 (2008).
  - <sup>20</sup> N. C. Mamani, G. M. Gusev, T. E. Lamas, A. K. Bakarov, O. E. Raichev, *Phys. Rev. B* **77**, 205327 (2008).
  - <sup>21</sup> A. A. Bykov, *JETP Lett.* **89**, 461 (2009).
  - <sup>22</sup> A. V. Goran, A. A. Bykov, A.I. Toropov, S. A. Vitkalov, *Phys. Rev. B* **80**, 193305 (2009).
  - <sup>23</sup> L. I. Magarill and A. A. Romanov, *Sov. Phys. Solid State* **13**, 828 (1971).
  - <sup>24</sup> V. M. Polyakovskii, *Sov. Phys. Semicond.* **22**, 1408 (1988).
  - <sup>25</sup> M. E. Raikh, T. V. Shahbazyan, *Phys. Rev. B* **49**, 5531 (1994).
  - <sup>26</sup> O. E. Raichev, *Phys. Rev. B* **78**, 125304 (2008).
  - <sup>27</sup> M. G. Vavilov and I. L. Aleiner, *Phys. Rev. B* **69**, 035303 (2004).
  - <sup>28</sup> S. Wiedmann, G. M. Gusev, O. E. Raichev, A. K. Bakarov, and J. C. Portal, *Phys. Rev. B* **82** 165333 (2010).
  - <sup>29</sup> Scott Dietrich, S. A. Vitkalov, D. V. Dmitriev, and A. A. Bykov, *Phys. Rev. B* **85**, 115312 (2012).
  - <sup>30</sup> T. H. Sander, S. N. Holmes, and J. J. Harris, D. K. Maude and J. C. Portal, *Phys. Rev. B* **58**, 13856 (1998).
  - <sup>31</sup> V. V. Solovyev, S. Schmult, W. Dietsche, and I. V. Kukushkin, *Phys. Rev. B* **80**, 241310 (2009).
  - <sup>32</sup> J. Nuebler, B. Friess, V. Umansky, B. Rosenow, M. Heiblum, K. von Klitzing, and J. Smet, *Phys. Rev. Lett.* **108**, 046804 (2012).
  - <sup>33</sup> J. Shabani, Y. Liu, and M. Shayegan, *Phys. Rev. Lett.* **105**, 246805 (2010).
  - <sup>34</sup> Y. Liu, D. Kamburov, M. Shayegan, L. N. Pfeiffer, K. W. West, and K. W. Baldwin, *Phys. Rev. Lett.* **107**, 176805 (2011).
  - <sup>35</sup> Y. Liu et al., *Phys. Rev. Lett.* **107**, 266802 (2011).
  - <sup>36</sup> Scott Dietrich, Sean Byrnes, Sergey Vitkalov, D. V. Dmitriev, and A. A. Bykov *Phys. Rev. B* **85**, 155307 (2012).
  - <sup>37</sup> Scott Dietrich, Sean Byrnes, Sergey Vitkalov, A. V. Goran, and A. A. Bykov *Phys. Rev. B* **86**, 075471 (2012).
  - <sup>38</sup> Scott Dietrich, Sean Byrnes, Sergey Vitkalov, A. V. Goran, and A. A. Bykov, *Journal of Applied Physics* **113**, 053709 (2013).
  - <sup>39</sup> M. A. Mueed, D. Kamburov, M. Shayegan, L. N. Pfeiffer, K.W. West, K.W. Baldwin, and R. Winkler, *Phys. Rev. Lett.* **114**, 236404 (2015).